Current Biology 24, 1039–1049, May 19, 2014 ©2014 Elsevier Ltd All rights reserved http://dx.doi.org/10.1016/j.cub.2014.03.048

Article

Neural Pathways for the Detection and Discrimination of Conspecific Song in *D. melanogaster*

Alexander G. Vaughan,[1] Chuan Zhou,[1] Devanand S. Manoli,[2] and Bruce S. Baker[1,*]
[1]Janelia Farm Research Campus, HHMI, Ashburn, VA 20147, USA
[2]Department of Psychology, UCSF, San Francisco, CA 94122, USA

Summary

Background: During courtship, male *Drosophila melanogaster* sing a multipart courtship song to female flies. This song is of particular interest because (1) it is species specific and varies widely within the genus, (2) it is a gating stimulus for females, who are sensitive detectors of conspecific song, and (3) it is the only sexual signal that is under both neural and genetic control. This song is perceived via mechanosensory neurons in the antennal Johnston's organ, which innervate the antennal mechanosensory and motor center (AMMC) of the brain. However, AMMC outputs that are responsible for detection and discrimination of conspecific courtship song remain unknown.
Results: Using a large-scale anatomical screen of AMMC interneurons, we identify seven projection neurons (aPNs) and five local interneurons (aLNs) that outline a complex architecture for the ascending mechanosensory pathway. Neuronal inactivation and hyperactivation during behavior reveal that only two classes of interneurons are necessary for song responses—the projection neuron aPN1 and GABAergic interneuron aLN(al). These neurons are necessary in both male and female flies. Physiological recordings in aPN1 reveal the integration of courtship song as a function of pulse rate and outline an intracellular transfer function that likely facilitates the response to conspecific song.
Conclusions: These results reveal a critical pathway for courtship hearing in male and female flies, in which both aLN(al) and aPN1 mediate the detection of conspecific song. The pathways arising from these neurons likely serve as a critical neural substrate for behavioral reproductive isolation in *D. melanogaster*.

Introduction

Courtship in *Drosophila melanogaster* is a sequence of innate behaviors that exchange multisensory cues between the sexes [1–4]. During courtship, a male fly identifies and orients toward the female using olfactory and visual cues, uses gustatory cues to determine sex and species, and sings a courtship song to elicit female receptivity before attempting copulation (Figure 1A). The female relies on chemosensory and auditory cues in choosing to mate with or reject the courting male. Courtship song is a particularly interesting sexual signal because, alone among sexual signals in *D. melanogaster*, its production and detection are under neuronal control [6, 7]. Although fly courtship has become a major model system for behavioral neurogenetics, we lack a functional understanding of the central circuits underlying the production of and response to these cues.

D. melanogaster song contains two signals: a hum-like sine song and a pulse song consisting of pulses at a ~35 ms interpulse interval (IPI; Figure 1A) [8]. Closely related species differ in major aspects of courtship song, including pulse types, mean IPI and intrapulse frequency (IPF) of pulse song, and the presence and frequency of sine song [2, 9]. Pulse song is the dominant auditory cue during courtship in *D. melanogaster*, whereas sine song may play a secondary role [6, 10–16]. In female flies, IPI is a critical determinant of receptivity and reinforces reproductive isolation between sympatric species [10, 12, 15]. Males are also sensitive to pulse song and respond to conspecific IPIs with increased locomotion and investigation of nearby flies [17–21]. Nevertheless, the neuronal pathways necessary for detecting courtship song, discriminating conspecific song, and regulating sexually dimorphic responses to song are essentially unknown.

Song perception is mediated by the Johnston's organ (JO) in the second antennal segment, in parallel with other mechanosensory cues [22]. For acoustic stimuli, near-field particle velocity signals (movement of bulk air rather than a pressure wave) impinge on the brush-like arista. This movement applies torque to the third antennal segment, which rotates around the funicular joint; chordotonal JO neurons (JONs) are attached at their distal end to the funicular hook and are dynamically stretched and relaxed by this motion. Gravitational, inertial, and wind stimuli move the third antennal segment directly, causing static deflections that stimulate distinct JON populations [20, 23]. As in mammalian hair cells, active processes mediate the frequency sensitivity of the auditory organ, and the spectral response properties of both JONs and some interneurons vary as a function of stimulus intensity or species [9, 22, 24].

The ~500 JONs within an antenna vary in their response to auditory and vestibular inputs as a function of their physiology and placement within the JO [9, 25]. Recent assays have sought to classify the response profiles of JON subpopulations [20, 23] and have suggested a model of mechanosensory architecture in which biomechanically and physiologically similar JONs converge onto modality-specific pseudoglomeruli in the antennal mechanosensory and motor center (AMMC); these regions are denoted as AMMC zones A–E (lateral to medial; Figure 1B) [25]. Although many biomechanical processes modulate antennal sensitivity, they do not explain the behavioral sensitivity to conspecific IPI in *D. melanogaster* [9, 22]. In particular, because the 35 ms pulse interval is much longer than the expected timescales of antennal resonance and JON integration, decoding of conspecific song is likely to rely on central neuronal mechanisms.

The many sex- and species-specific aspects of courtship hearing suggest a role for the sex-determination hierarchy, and in particular the terminal genes *fruitless* (fru^M) and *doublesex* (*dsx*) that specify many aspects of courtship behavior [3]. Expression of fru^M has been identified in JONs and some candidate central auditory neurons, but the nature of the sexual dimorphism in the auditory pathway is unclear [26–30].

*Correspondence: bakerb@janelia.hhmi.org

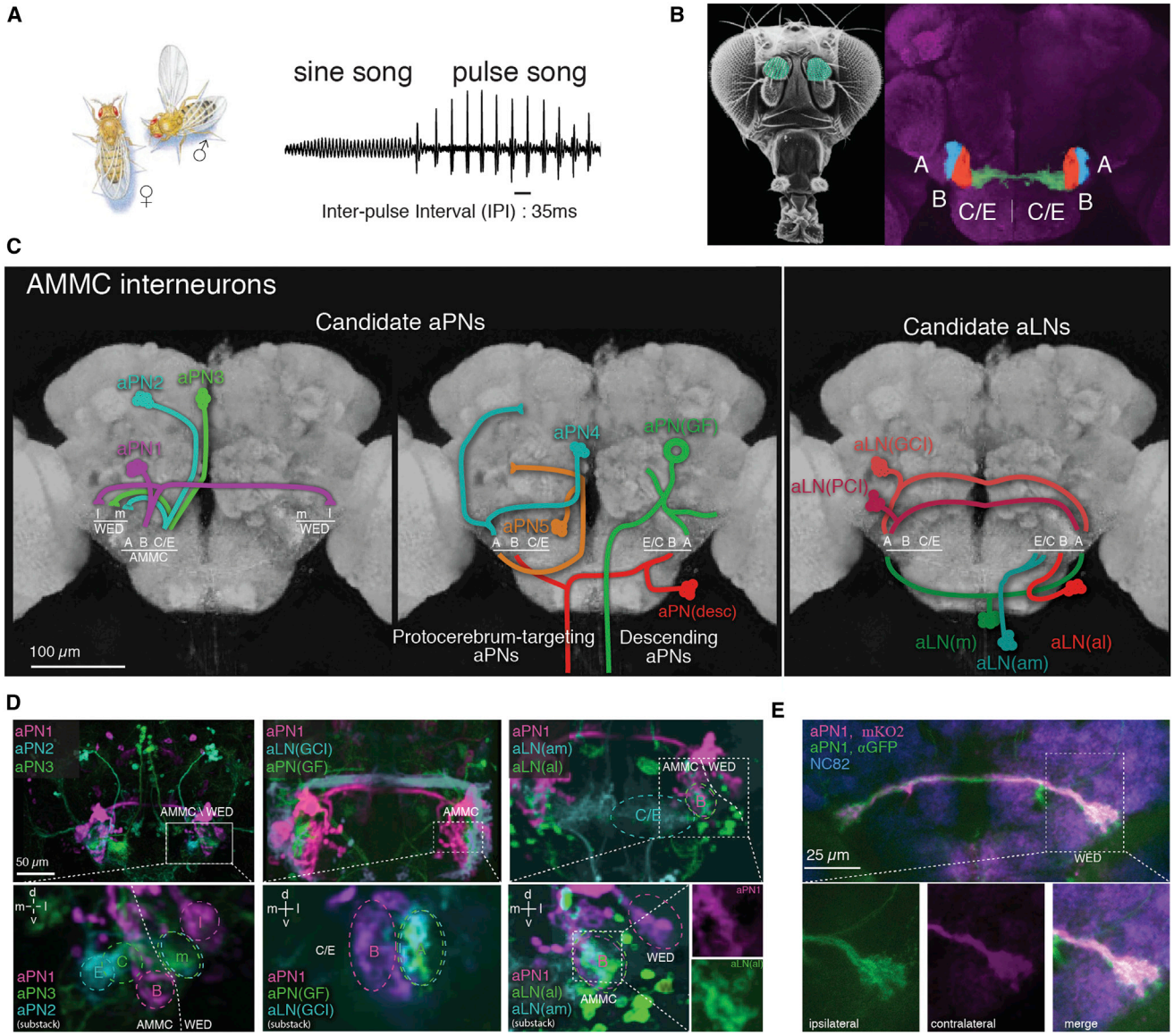

Figure 1. Cellular Architecture of Afferent Mechanosensory Pathway

(A) Courtship song, sung by the male fly toward the female, consists of both sine song and pulse song, with an average interpulse interval (IPI) of 35 ms.
(B) Courtship song and other mechanosensory stimuli are received by Johnston's organ neurons (blue, left) that project to discrete AMMC zones A–E.
(C) Schematic projections of twelve identified classes of AMMC interneuron, including seven classes of candidate aPNs (left) and five classes of aLNs (right).
(D) Arborization of aPNs and aLNs in AMMC and projection areas in female flies, visualized by whole-brain registration. Left: aPN1 projects from AMMC zone B to the lateral WED, while aPN2 and aPN3 project from AMMC zone C/E to medial WED. Center: aPN1 arborization in AMMC zone B is distinct from aPN(GF) and aLN(GCl) arborization in AMMC zone A. Right: arborization of aPN1 in AMMC zone B overlaps with aLN(al), but not aLN(am). The CRM lines used were as follows: aPN1: R63A03; aPN2: R24C06; aPN3: R70G01; aLN(GCl): R11A07; aLN(GF): R79D08; aLN(al): R25B01; aLN(am): R19E09.
(E) Clonal analysis of aPN1 generated using R45D07 and dBrainbow shows overlap of ipsilateral and contralateral projections in WED (αGFP, green; mKO2, magenta; NC82, blue; 10 μM section).
Drosophila illustration from [5]. See also Figure S1.

Several identified AMMC interneurons may play a role in auditory or vestibular processing, including a subset that express *fru*^{M} [20, 24, 28, 29, 31, 32]. Identification of these neurons has led to several hypothetical circuit architectures, including the suggestion that auditory cues are processed in the brain while vestibular cues are routed directly to the ventral nerve cord (VNC) [20] and the hypothesis that pathways for courtship hearing may be mediated by *fru*^{M}-expressing interneurons [28–30].

Physiological recordings have provided some insight into the pathways for courtship hearing, with the surprising result that at least six distinct cell types respond to either pulse song or sine song, including AMMC-B1, AMMC-A2, IVLP-IVLP PN, AMMC-A1, AMMC-B2, and the giant fiber (see Table S2 available online for correspondence to the driver lines used in this work) [29, 32]. In particular, because pulse song responses have been observed in essentially every cell type tested, it seems unlikely that physiological recordings alone will suffice to identify the true basis of courtship hearing. Moreover, no assays have been performed that demonstrate the necessity of any cell type for courtship hearing in either sex.

For a more complete understanding of the neural circuit underlying courtship hearing, an integrated approach is required.

Here, we aimed to provide this integrated approach by identifying and interrogating the circuitry underlying courtship song responses in *D. melanogaster* males and females. We conducted a visual screen of ~6,000 GAL4 lines with expression in the CNS and identified seven major classes of candidate auditory projection neurons (aPNs) and five classes of auditory local neurons (aLNs), which span the anatomical extent of the AMMC and provide for divergent afferent pathways for mechanosensation to a variety of downstream regions (Figures 1C and S1). In particular, these projections are highlighted by ascending projections to the wedge (WED) from AMMC neuropiles associated with both acoustic and vestibular cues, defining a major new multisensory pathway.

Identification of these cell types, including eight types not previously reported or known only from clonal analysis, allows the direct manipulation of a large fraction of the AMMC circuitry for the first time (Tables S1 and S2). Using complementary assays in male and female flies, we tested each interneuron class for its role in courtship hearing. Surprisingly, we observed that only one class of projection neurons (aPN1) and one class of local interneurons (aLN(al)) are necessary for behavioral responses to song in either sex. Strikingly, at least a subset of neurons in both cell types express fru^M and may serve as a "labeled line" carrying courtship song information from the AMMC to WED.

Direct GCaMP recordings in aPN1 reveal integration of pulse song across a broad range of IPIs, with a robust response to conspecific and heterospecific song. Moreover, a comparison of dendritic and axonal responses reveals an intracellular band-pass filter that may assist in both detection and discrimination of conspecific song.

Results

Identification of Candidate Afferent Auditory Neurons

Using the JFRC FlyLight collection, we screened ~6,000 *cis*-regulatory module (CRM)-GAL4 lines for expression in the AMMC [33]. We identified 288 lines with selective AMMC expression and categorized these into five classes of aLNs and seven classes of aPNs (Figures 1C and S1; see also Tables S1 and S2 and Supplemental Experimental Procedures). Each class was identifiable in an average of 14 CRM lines, suggesting deep coverage. We selected a subset of driver lines for further study that provided robust expression while limiting off-target expression (Table S3).

Several of the aPN/aLN cell types described here are related to neurons previously identified by GAL4 lines, clonal analysis, or fru^M expression. Of particular note, the aPN1 nomenclature used here integrates overlapping cell types previously described as AMMC-B1, AMMC-IVLP PN1, AMMC-2–AMMC-8, AMMC-10, and AMMC-11, as well as the fru^M-expressing subset aDT-e [20, 28, 29, 31]. Similarly, the aLN(al) cell type corresponds to AMMC LN and the fru^M-expressing neuron *pSG-a* [28, 29]. See Table S2 for a unified nomenclature of these cell types.

We assayed the morphology and directionality of aPN and aLN cell types as well as the expression of the inhibitory neurotransmitter gamma-aminobutyric acid (GABA) and the sex-determination gene fru^M. Projection neurons vary in arborization targets outside the AMMC and show two major pathways of parallel multilineage projections: aPN1, aPN2, and aPN3 project in parallel from AMMC to WED, while aPN(GF) and aPN(desc) descend to premotor regions of the VNC.

We used whole-brain registration of CRM lines to clarify the relative arborization of each neuronal class within the AMMC and projection regions (Figure 1D) [34]. These results reveal a tiling of the AMMC by aPN and aLN arbors with discrete zones of arborization in AMMC regions associated with startle (zone A: aPN(GF), aPN4, aPN5, aLN(GCl), aLN(m), and aLN(PCl)), acoustic (zone B: aPN1, aPN(desc), aLN(al), aLN(m), and aLN(PCl)), and vestibular responses (zone C/E: aPN2, aPN3, and aLN(am)) [20, 23, 29]. Notably, we did not observe a bifurcation of putative auditory and vestibular pathways [20] but instead identified a multilineage pathway carrying information from AMMC in which bilateral inputs from aPN1 and ipsilateral inputs from aPN2 and aPN3 converge in the lateral and medial WED (Figures 1D, 1E, and S1G). This suggests that WED serves as a major site for multimodal mechanosensation.

Histological examination of the aPN and aLN populations reveals a population of excitatory ascending aPNs modulated by GABAergic aLNs. When expressing SYT::HA and DSCAM::GFP as presynaptic and postsynaptic markers, aPN1 and aPN2 showed clear AMMC-WED polarity, while aPN3 showed SYT:HA staining in both AMMC and WED and may participate in bidirectional signaling (Figure S1C) [28]. aPN4, aPN5, and aPN(desc) showed patterns consistent with ascending projections from AMMC to other regions (data not shown). Antibody staining revealed GABA expression in aLN cell types, but not in aPNs (Figure S1D and Table S1). These results reveal an architecture in which aPNs innervating the AMMC in tiled areas are largely ascending and excitatory and modulated by largely inhibitory aLN signals.

Several putative auditory interneurons may express fru^M [28–30]. Using the $fru^{P1.LexA}$ reagent, we confirmed the expression of fru^M in the aPN1, but not aPN2 or aPN3, neurons (Figures S2E and S2F). Comparison of our own clonal analysis of aPN and aLN populations allowed a direct comparison to neurons identified using fru^M reporters: overall, we note fru^M expression in at least five cell types, with varying arborization in AMMC and target areas (Table S2) [28, 30]. We did not observe gross sexual dimorphism in these cell types, but we cannot rule out dimorphism in the subset of fru^M-expressing neurons in each lineage (data not shown).

The set of aPN and aLN cell types identified here reveals the considerable complexity of the AMMC circuit. Within each pseudoglomerular region of the AMMC, distinct classes of inhibitory aLNs and excitatory aPNs may allow for segregated processing of distinct mechanosensory cues. Many of these cell types are candidates for a role in courtship hearing based on anatomy, expression of fru^M, and responsiveness to pulse song [28–30, 32]. To identify which of these cell types are necessary for courtship behavior, we turned to behavioral manipulations in male and female flies.

Behavioral Assays for Courtship Hearing

Female receptivity (FR) in *D. melanogaster*, measured as the latency to copulation, is reliably disrupted by manipulations of courtship hearing (Figure 2A) [4]. In our hands, silencing male flies by removing their wings or deafening female flies by removing their aristae significantly increased the time to mating (Cox proportional hazards test: $p < 0.002$ and $p < 0.006$; Figure 2B). Similarly, $shibire^{TS}$-mediated silencing of all JONs or all fru^M-expressing antennal neurons decreased receptivity (Cox proportional hazards ANOVA,

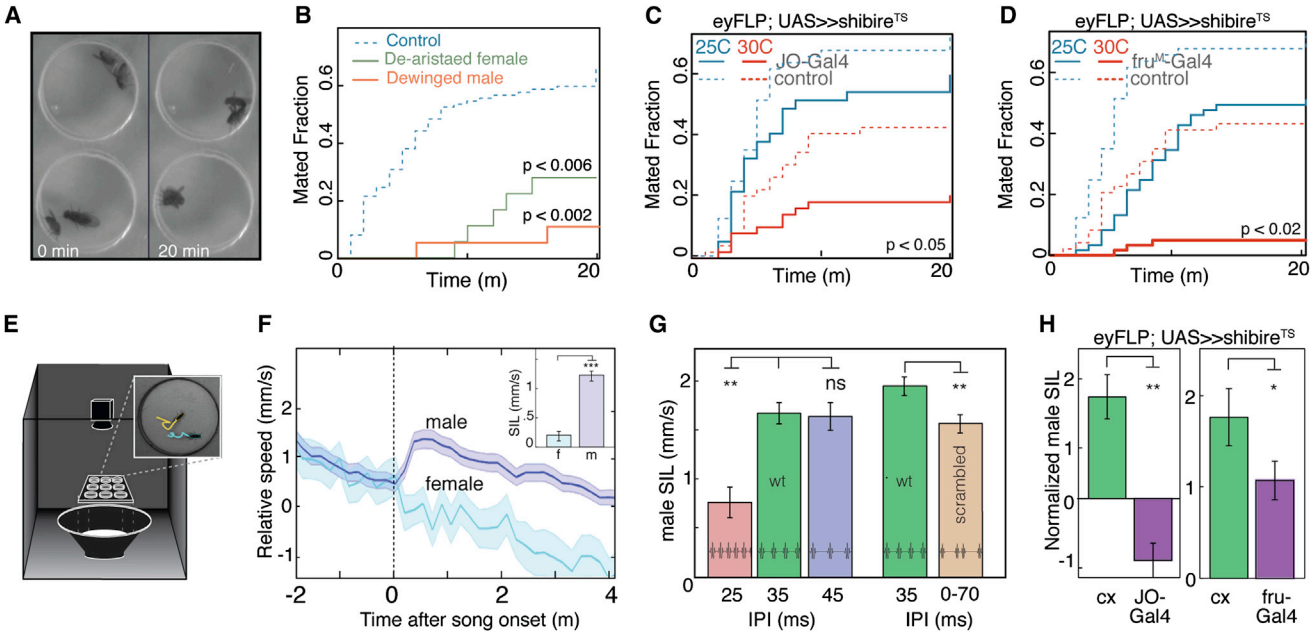

Figure 2. Neuronal Silencing in aPN1 and aLN(al) Disrupts Courtship Hearing in Both Male and Female Flies

(A) The FR assay. Mating success is measured over a 20 min interval.

(B) FR is reduced by disruption of courtship hearing by removal of male wings (Cox proportional hazards test: $p < 0.002$ versus wild-type flies) or the female aristae ($p < 0.006$).

(C and D) FR is significantly reduced by *shibire*^{TS}-mediated silencing of all JONs (genotype × temperature interaction, Cox proportional hazards ANOVA: $p < 0.02$, C) or *fru*^{M} antennal neurons ($p < 0.02$, D).

(E) The SIL assay. The locomotor response to courtship song is observed in pairs of male flies.

(F) Males, but not females, increase in speed in response to pulse song (t test versus no increase: males, $p < 0.01$; females, $p > 0.5$).

(G) Male SIL is reduced at short, but not long, IPIs (t test versus response at 35 ms IPI: 25 ms, $p < 0.01$; 45 ms, $p < 0.44$, left) and is also reduced by song with a mean 35 ms IPI but high variability in IPI (t test for "scrambled song" versus 35 ms IPI, $p < 0.01$, right).

(H) Male SIL response is reduced by *shibire*^{TS}-mediated silencing of JONs (genotype × temperature interaction, two-way ANOVA: $p < 0.01$, left) or *fru*^{M} antennal neurons ($p < 0.03$, right). For *shibire*^{TS} manipulations in both FR and SIL assays, a reduction in FR or SIL is reported as a significant genotype × temperature interaction term in a two-way ANOVA (for FR, a Cox proportional hazards ANOVA). Permissive temperatures and the empty-GAL4 driver BDPG4U were used as controls. For SIL data, results are presented graphically as the normalized increase in speed for each genotype (i.e., $SIL_{29.5°C}/SIL_{25°C}$). Error bars show mean ± SEM; *$p < 0.05$, **$p < 0.01$, ***$p < 0.001$.

genotype × temperature interaction: R61D08, $p < 0.02$; *fru*^{GAL4}, $p < 0.02$; Figures 2C and 2D). However, because this assay depends strongly on sensory cues and internal states that are difficult to control, it must be supplemented with a complementary assay in male flies.

In male flies, courtship song stimuli increase locomotion and the investigation of other flies [19, 21]. Based on this work, we developed a robust assay for male song-induced locomotion (SIL) in response to synthetic pulse song that directly quantifies the locomotor response of pairs of male flies (Figures 2E–2H; see Supplemental Experimental Procedures). We validated the SIL response as a quantitative measure of male courtship hearing by three criteria. First, the SIL response is sex specific: male flies increase in average speed in response to synthetic pulse song (~1.5 mm/s), whereas females do not (t test versus no response, males: $p < 0.01$; females: $p > 0.5$; Figure 2F). Second, male SIL requires high-quality and species-appropriate song stimuli, and females show diminished responses to song with short IPIs (t test versus 35 ms IPI control: 25 ms IPI, $p < 0.01$; 45ms IPI, $p < 0.5$) as well as a reduced response to "scrambled" song with high variability (t test versus wild-type song: $p < 0.01$; Figure 2G). This asymmetrical "low-pass" response to pulse song has been observed previously [19]. Third, the SIL response requires antennal hearing: neuronal silencing of all JONs by *shibire*^{TS} or all *fru*^{M} neurons in the eye-antennal disc significantly reduced the male SIL response (two-way ANOVA, genotype × temperature interaction: JO-GAL4, $p < 0.01$; *fru*^{GAL4}, $p < 0.03$; Figure 2H).

Together, these results suggest that SIL is a sensitive assay for courtship hearing and that this response is sex specific, requires antennal hearing, and is sensitive to high-quality conspecific song. Alongside FR, this assay provides the basis for a careful examination of the role of aPNs and aLNs in courtship hearing in both sexes.

Neuronal Silencing in Candidate Auditory Interneurons

We next sought to identify which aPN populations were necessary for courtship hearing in either male or female flies by testing all seven aPN cell types in both the FR and SIL assays under *shibire*^{TS}-mediated silencing. Remarkably, only silencing of aPN1 reliably generated courtship-hearing deficits in either sex in these assays (Figures 3A–3E). Using four distinct drivers for aPN1, we observed consistent disruption of FR (R45D07, $p < 0.03$; R59C10, $p < 0.005$; R63A03, $p < 0.01$; R22B11, $p < 0.03$; Figures 3B–3E, left panels). In male flies, three of the four drivers also showed significant disruption of SIL (R45D07, $p < 0.001$; R59C10, $p < 0.03$; R63A03, $p < 0.03$, R22B11, $p < 0.3$; Figures 3B–3E, right panels).

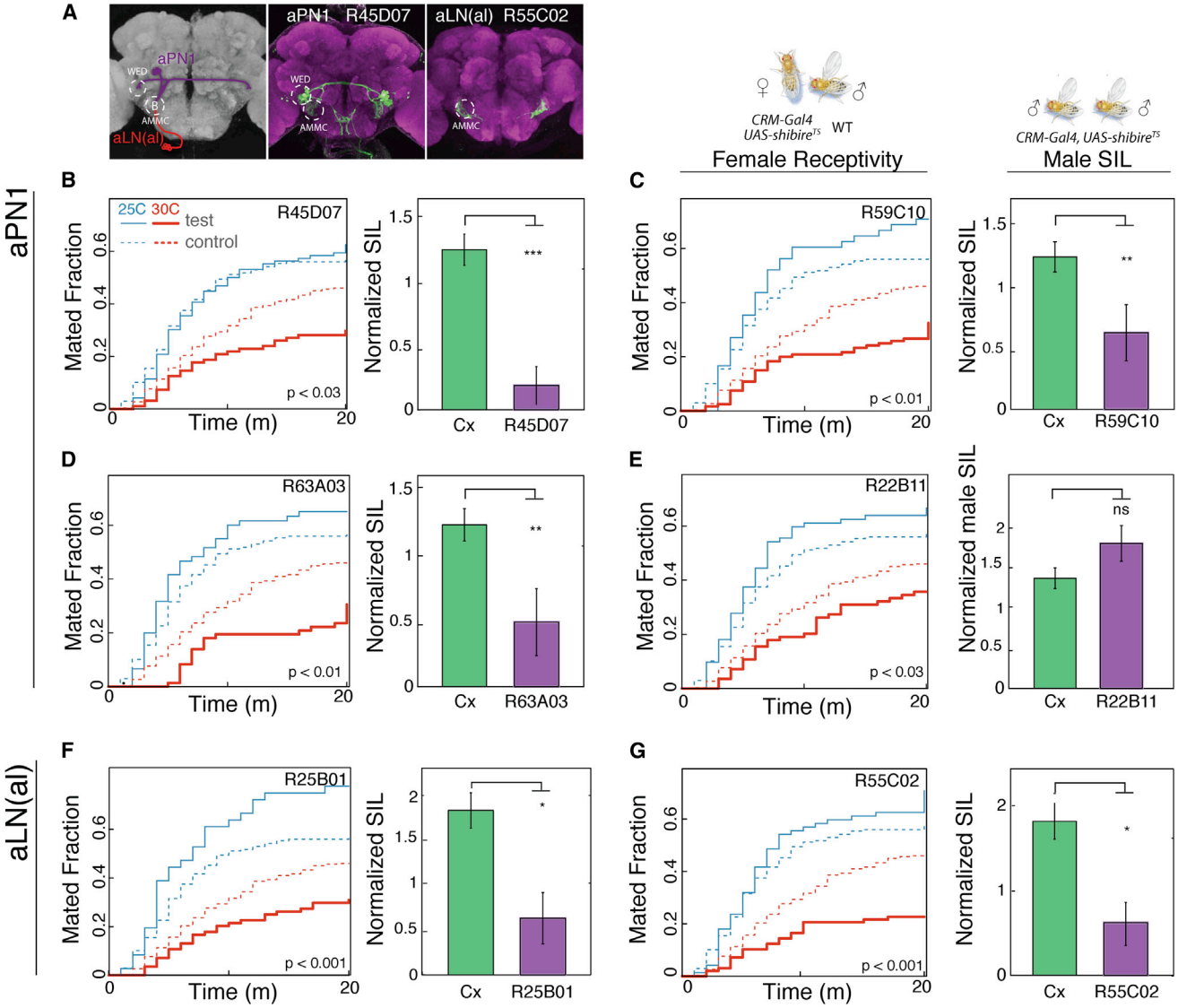

Figure 3. Neuronal Silencing of aPN1 and aLN(al) Disrupts Courtship Hearing

(A–G) Neuronal silencing mediated by expression of *shibire*^{TS} was targeted to aPN1 and aLN(al) using several independent CRM-GAL4 driver lines, and each line was tested for disruption of FR (left panels) and male SIL (right panels).

(A) Arborization of driver lines for aPN1 (R45D07, center) and aLN(al) (R55C02, right) in AMMC and WED.

(B–E) Neuronal silencing of aPN1 using *shibire*^{TS}- driven by several independent GAL4 drivers significantly disrupted both FR and male SIL (R45D07, B; R59C10, C; R63A03, D; and R22B11, E). All four drivers tested showed significant disruption of FR when driving *shibire*^{TS}-mediated silencing, while all except R22B11 also disrupted male SIL (E).

(F and G) Neuronal silencing of aLN(al) using two distinct drivers disrupts both FR and male SIL (R25B01, F; R55C02, G).

Statistics were performed as for Figure 2; see Table S4 for full behavioral results. Error bars show mean ± SEM; *p < 0.05, **p < 0.01, ***p < 0.001.

Neuronal silencing of other aPN classes, in both male and female flies, revealed no consistent effects on courtship hearing (Figures 4A–4H). We did note one possible phenotype using a driver for aPN3 in which neuronal silencing disrupted FR (R70G01, $p < 0.03$; Figure 4B, left). However, this observation was not replicated for male SIL (R70G01, $p < 0.22$ for SIL; Figure 4B, right) or for FR using an independent driver (R30A07, $p < 0.22$ for FR, $p < 0.8$ for SIL; Figure 4C) and is thus likely to arise from off-target expression in R70G01. Thus, among AMMC projection neurons, only aPN1 appears to be necessary for courtship hearing in either male or female flies (see also Table S4).

Neuronal silencing in aLNs revealed similar selectivity: silencing of one aLN cell type—aLN(al)—disrupted courtship hearing in both sexes (R25B01, $p < 0.001$ for FR, $p < 0.02$ for SIL; R55C02, $p < 0.001$ for FR, $p < 0.02$ for SIL; Figures 3F and 3G). Neuronal silencing had no effect on FR or male SIL in any other class of aLNs ($p > 0.05$ for all driver lines in both FR and SIL; Figures 4I–4L).

These results largely align with two previous organizing principles for courtship hearing. In the AMMC, aPN1 and aLN(al) arborize within zone B, a region previously implicated in mediating the response to courtship song [20]. In addition, at least a subset of neurons in each population known to be necessary for courtship hearing (i.e., JONs, aPN1, and aLN(al)) express

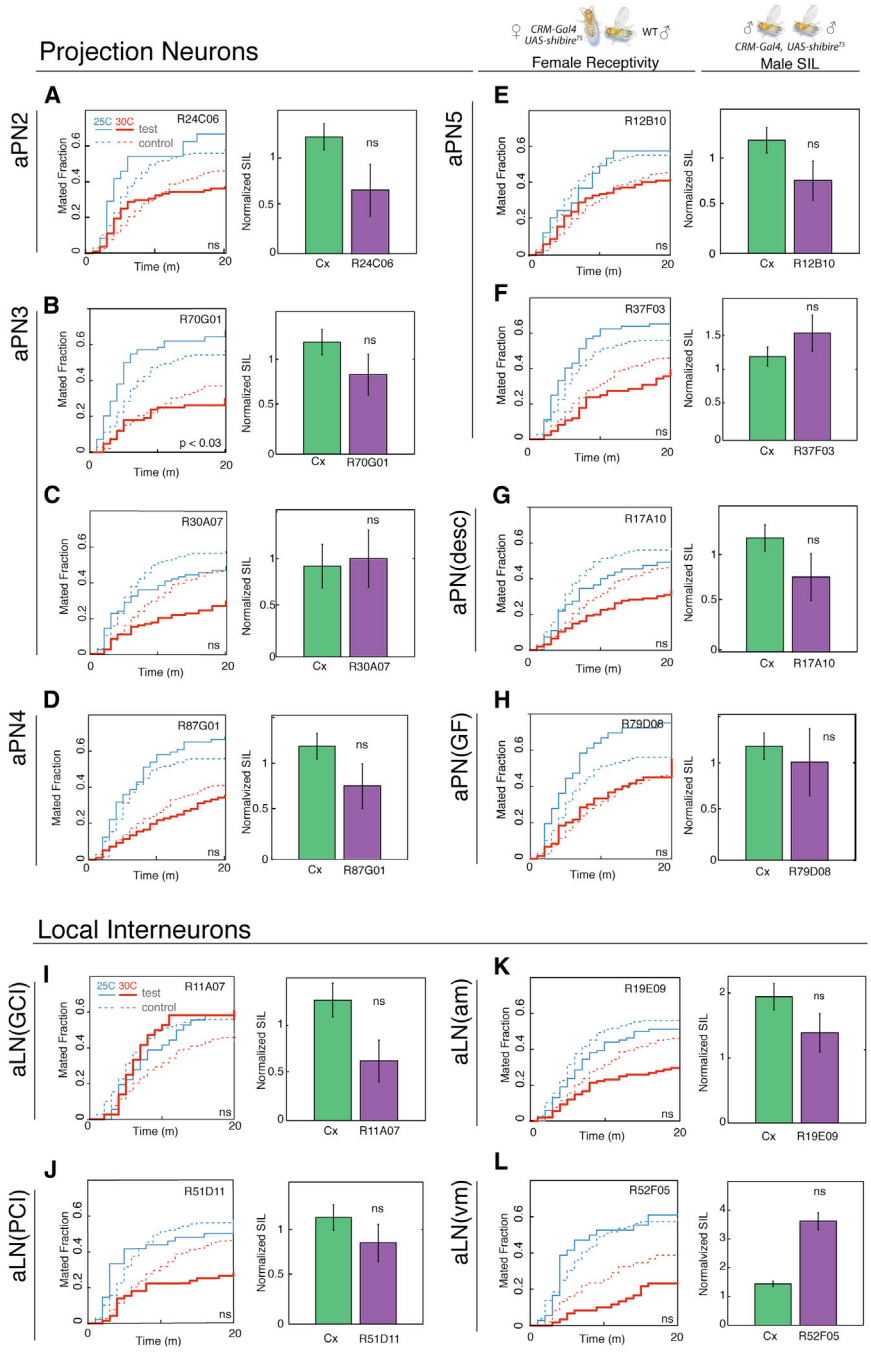

Figure 4. Neuronal Silencing of Other aPNs and aLNs Has No Effect on Courtship Hearing

(A–H) Neuronal silencing in candidate aPNs (other than aPN1) had no reliable effect on FR (left panels) or male SIL (right panels). For most putative cell types and driver lines tested, neuronal silencing had no effect on FR or male SIL (aPN2: R24C06, A; aPN3: R70G01, R30A07, B and C; aPN4: R87G01, D; aPN5: R12B10, R37F03, E and F; aPN(desc): R17A10, G; aPN(GF): R79D08, H). Neuronal silencing in aPN3 using one driver generated a significant reduction of FR, but not male SIL (R70G01, B); this effect was not replicated using another aPN3 driver (R30A07, E).

(I–L) Neuronal silencing in other candidate aLNs had no effect on courtship hearing in FR or male SIL (aLN(GCl): R11A07, I; aLN(PCl): R51D11, J; aLN(am): R19E09, K; aLN(m): R52F05, L). For SIL and FR, genotype × temperature interactions were identified by ANOVA as for Figure 2.

See Table S4 for full behavioral results. Error bars show mean ± SEM; *p < 0.05, **p < 0.01, ***p < 0.001.

the sexually dimorphic transcription factor *fru*^{M} (see Tables S1 and S2). We note that other candidate auditory interneuron classes showing *fru*^{M} expression (aPN5, aPN(desc), and aLN(m)) appear to be dispensable for courtship hearing, at least in these assays.

Hyperactivation of Candidate Auditory Interneurons

We next examined the effects of *dTrpA1*-mediated hyperactivation on courtship hearing. In doing so, we sought to examine two issues. First, we sought to confirm that the specificity of the silencing result, which identifies aPN1 and aLN(al) alone as necessary for courtship hearing, was not an artifact of the *shibire*^{TS} manipulation or of neuronal architecture. For example, silencing a neuron involved in gating inhibition would not disrupt a circuit response, but hyperactivation of the same neuron may do so. Second, we sought insight into potential encoding schemes for courtship song in aPN1 and aLN(al). We note that in many cases, including pheromonal gustation [35], olfaction [36], courtship [37], and aggression [38], tonic hyperactivation and silencing have opposite effects. From these results, we reasoned that neuronal hyperactivation in aPNs may provide a fictive song stimulus even in the absence of natural song, which would imply that the presence or quality of courtship song is represented as a rate code. In contrast, should hyperactivation disrupt courtship hearing, this would suggest a more temporally complex representation of courtship song that is sensitive to disruption.

To confirm the specificity of *shibire*^{TS} silencing, we tested the effect of *dTrpA1* hyperactivation on FR. For both aPN1 and aLN(al), hyperactivation dramatically reduced FR to wild-type males (aPN1: R45D07, $p < 0.001$; R59C10, $p < 0.001$; aLN(al): R25B01, $p < 0.01$; Figures 5A, 5B, and 5I). There was no effect on FR when hyperactivation was targeted to other aPN/aLN cell types ($p > 0.05$ for all cell types; Figures 5C–5H and 5J–5M).

To test whether hyperactivation could serve as a fictive song stimulus, we tested whether hyperactivation of aPNs increased FR toward wingless (and thus muted) males. Consistent with the selectivity of the aPN1 response and the reduction in receptivity toward intact males seen in aPN1-*dTrpA1* flies, hyperactivation of aPN1, aPN2, or aPN3 failed to restore receptivity in females (aPN1: R59C10, $p < 0.3$; aPN2: R24C06, $p < 0.3$; aPN3: R70G01, $p < 0.7$; Figures 6A–6C).

These results reinforce the observation that the aPN1/aLN(al) pathway is critical to courtship hearing in female flies

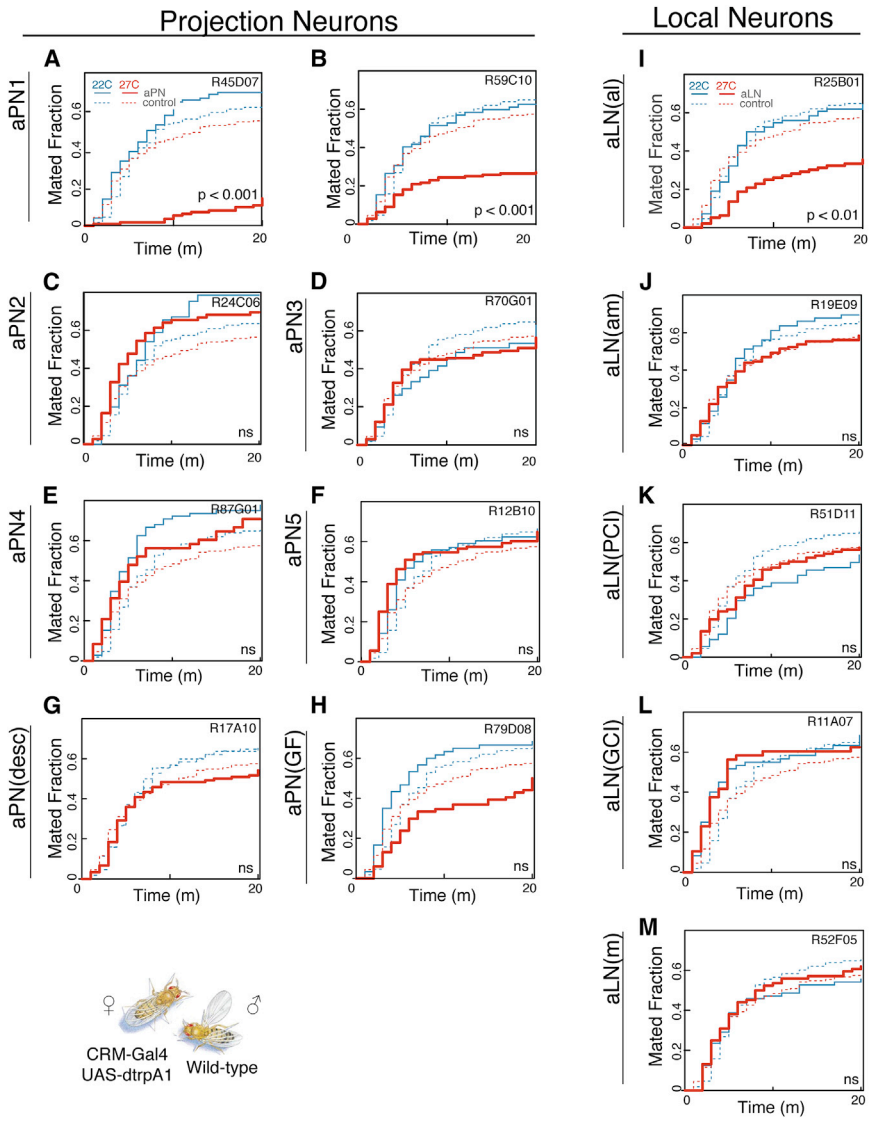

Figure 5. Hyperactivation of aPN1/aLN(al) Decreases FR

(A and B) *dTrpA1*-mediated hyperactivation of aPN1 significantly reduced FR (R45D07: $p < 0.001$, A; R59C10: $p < 0.001$, B).

(C–H) Outside of aPN1, *dTrpA1*-mediated hyperactivation had no effect on FR toward intact male flies (aPN2: R24C06, C; aPN3: R70G01 D; aPN4: R87G01, E; aPN5: R12B10, F; aPN(desc): R17A0, G; aPN(GF): 79D08, H).

(I) *dTrpA1*-mediated hyperactivation in aLN(al) significantly reduced FR (R25B01: $p < 0.01$).

(J–M) Hyperactivation of other aLNs had no effect on FR (aLN(am): R19E09, J; aLN(PCl): R11A07, K; aLN(GCl): R51D11, L; aLN(m): R52F05, M).

Statistics were performed as for Figure 2; see Table S4 for full behavioral results. *$p < 0.05$, **$p < 0.01$, ***$p < 0.001$.

and suggest that a temporally complex representation of courtship song in aPN1 is carried to downstream areas for further processing. To understand these representations in more detail, we directly visualized the aPN1 response to courtship song using GCaMP imaging.

The Response of aPN1 to Pulse Song

We tested the response of aPN1 to pulse song using GCaMP3, expressed via the R45D07 driver and imaged through a ventral window to allow simultaneous visualization of dendritic (AMMC) and axonal (WED) fields (Figures 7A and 7B) [39]. In the AMMC, we observed a strong GCaMP response to synthetic pulse song; by varying stimulus intensity and duration over a wide range, we identified a stimulus within the linear response range for further analysis (90 dB sound particle velocity level [SPVL], 40 pulses per train; $\Delta F/F$ defined as $F_{post} - F_{pre}/F_{pre}$; Figures 7C and 7D).

Using this stimulus, we examined how the aPN1 GCaMP response varied as a function of IPI. We first tested the response of aPN1 to varying IPIs in the AMMC and observed that peak $\Delta F/F$ varied linearly across a wide range of pulse rates (i.e., as 1/IPI) but was significantly attenuated at the shortest IPI tested (F test for linear fit between 25 and 65 ms IPI: $R^2 = 0.48$, $p < 0.001$; t test for response at 20 ms IPI versus linear expectation: $p < 10^{-5}$; Figure 7E). Because the stimuli used are well within the linear response range for the AMMC response, this attenuation is likely to reflect the response properties of aPN1 or innervating JONs rather than saturation of antennal biomechanics or the GCaMP signal (Figures 7C and 7D). In comparison to the AMMC response, the GCaMP signal in WED appeared somewhat less linear but still showed a similar integration between 25 and 65 ms IPI (linear fit: $R^2 = 0.45$; $p < 0.001$) as well as a significant attenuation at 20 ms IPI (t test versus linear expectation: $p < 10^{-6}$; Figure 7F).

The aPN1 response to pulse song effectively integrates pulse rate, with a diminished response to 20 ms IPI that likely indicates significant filtering somewhere between JON activation and its input to aPN1. Notably, although a variety of AMMC interneurons have been reported to respond to pulse song and/or sine song, this result identifies the first evidence for IPI-sensitive responses to pulse song in any interneuron.

To compare AMMC and WED responses more directly, we exploited our strategy of simultaneous recordings in AMMC and WED to allow a direct comparison of the aPN1 response in these dendritic and axonal compartments. We first plotted the AMMC and WED signals observed in each fly across a range of IPIs, normalized by the average responses at 65 ms IPI (Figure 7G). This analysis revealed a nonlinear relationship between dendritic and axonal GCaMP signals, with a surprising suppression of the axonal GCaMP signal at short IPIs. This relationship was well described by the Hill equation, a damping function that has been identified as a common feature of many early sensory systems [40, 41]. We modeled WED output (W) as a function of AMMC input (A) as $W = a(A^b)/(A^b + c^b)$, where a–c are fit parameters. For aPN1, this function was well fit as $W = 1.66 \times (A^{8.3})/(A^{8.3} + 1.01^{8.3})$ (F test versus linear total least squares fit: $R^2 = 0.85$, $p = 0.001$). This interpretation represents

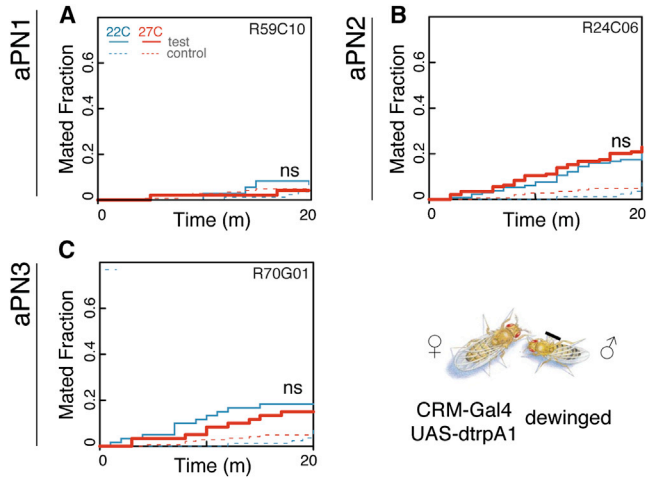

Figure 6. aPN Hyperactivation Fails to Rescue FR to Mute Males

(A–C) Hyperactivation of aPN1 (R59C10, A), aPN2 (R24C06, B), or aPN3 (R70G01, C) by *dTrpA1* did not significantly increase receptivity toward dewinged males, although these males still showed high levels of courtship. Statistics were performed as for Figure 2; see Table S4 for full behavioral results.

a saturation step within a larger-gain control or contrast response function.

We next calculated the AMMC-WED transfer function, which reveals the range of IPI responses that are amplified or suppressed at some point between aPN1 input in AMMC and output in WED. This intracellular transfer function revealed significant selectivity toward conspecific song: the WED response to pulse song with a 35 ms IPI was significantly greater than the response to song with both shorter and longer IPIs (one-way ANOVA: $p < 0.03$; Tukey's LSD comparison to 35 ms IPI: 25 ms IPI, $p < 0.03$; $p < 0.03$ for all IPIs between 45 and 65 ms; Figure 7H). This response is unlikely to be an artifact of biased sampling of finite-duration stimuli across the GCaMP integration window (Figure S2). Critically, this analysis suggests that, in addition to integrating pulse rate at the site of AMMC inputs, aPN1 may serve as a band-pass filter for IPI favoring the transmission of conspecific song.

These experiments suggest a complex role for aPN1 in courtship song processing. At a gross level, aPN1 appears to integrate pulse song in direct proportion to pulse rate. However, this response is modified by a two-stage filtering process. First, the response to pulse song with IPIs below ~25 ms is attenuated at or before the aPN1 dendritic field. Second, the transfer function between dendritic and axonal compartments supplies a weak band-pass filter favoring conspecific song near 35 ms IPI. Thus, although aPN1 neurons respond to pulse song over a broad IPI range, both aPN1 inputs and the intracellular aPN1 transfer function may serve as preprocessing filters for downstream identification of conspecific song.

Discussion

The Structure and Diversity of the AMMC Circuit

We identify twelve types of candidate mechanosensory neurons arborizing within the AMMC, including seven aPNs and five aLNs. Putative aPNs target widely disparate areas of the CNS but show striking parallel projections to WED arising from AMMC zones associated with acoustic (zone B: aPN1) and vestibular (zone C/E: aPN2 and aPN3) stimuli. Surprisingly, these parallel projections do not appear to support a common modality; aPN1 alone is necessary for courtship hearing, whereas aPN2 and aPN3 are dispensable (at least in these assays) and are hypothesized to underlie vestibular responses. Contrary to previous hypotheses of rapidly descending mechanosensory circuits, this revised architecture outlines the possibility of processing within the brain for each mechanosensory modality [20].

For the aPN1 cell type, we note that the drivers identified here do not resolve the possibility of anatomical or functional diversity within this sublineage. Indeed, aPN1 likely includes several subtypes that may be distinguished by functional [29], genetic [28], or anatomical criteria [31]. A detailed characterization of this diversity will be required to identify the limiting set that is necessary for courtship hearing in males or females.

Interestingly, expression of fru^M is observed in both aPN1 and aLN(al) cell types but also in other cell types not implicated in courtship hearing—aPN5, aPN(desc), and aLN(m). Their common arborization in AMMC zone A implicates these neurons in a startle response; we hypothesize that these neurons may respond to social stimuli with negative valence, such as aggression or female rejection signals [20, 28, 30], or to substrate-born vibration [42]. Further investigation will be required to understand the role of fru^M-expressing interneurons, in particular in the aPN1 and aLN(al) cell types, in processing mechanosensory social cues.

Encoding Song in the Afferent Auditory Pathway

What is the role of the early insect auditory system in processing courtship song? In a variety of species, a combination of biomechanical and physiological filters in the auditory organ, as well as central neuronal processing, may interact to discriminate both the frequency content and the temporal structure of courtship song [9].

In many cases, peripheral mechanisms can decode auditory cues without significant central processing. For example, chordotonal neuron physiology in Orthoptera allows for frequency discrimination of conspecific versus predatory sounds, whereas biomechanical innovations allow for phase-based localization in *Ormia* [43]. These mechanisms appear to derive behavioral sensitivity from the simple firing rate of the chordotonal neurons. Discrimination of temporal stimuli, such as pulse song IPI, may require more complex central processing.

One surprisingly similar model is the female cricket *Gryllus bimaculatus,* which shows phonotaxis to male calling song, carrying a species-specific interchirp interval (ICI) of ~35 ms [44]. The omega interneuron responds to calling song using a simple rate code for ICI—with a burst of spikes for each chirp. Although the omega interneuron largely integrates calling song as a function of chirp rate, the peak firing rate is attenuated at short ICIs. Stimuli that elicit high peak firing match the selective range of female phonotaxis, suggesting that the omega response serves as a band-pass filter facilitating discrimination of conspecific song.

Recordings in aPN1 suggest an analogous model. The dendritic GCaMP response shows a linear integration of pulse rate across a broad range but is suppressed at very low IPIs. Normalizing for this dendritic input, we observe that the axonal GCaMP signal favors the response to conspecific IPIs, suggesting that aPN1 activation serves as a supportive

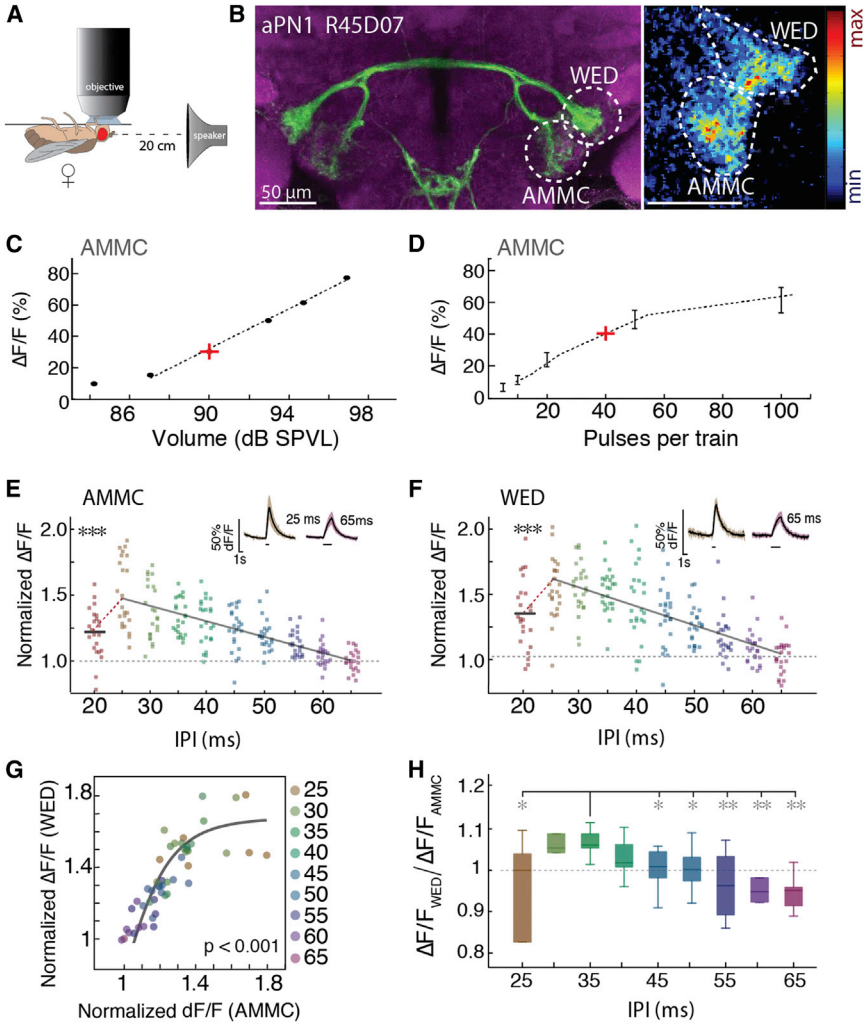

Figure 7. aPN1 Responds to Courtship Song

(A and B) Imaging setup (A) and recording sites (B) for GCaMP recording in dendritic (AMMC) and axonal (WED) fields of aPN1.

(C) GCaMP response of aPN1 in the AMMC. ΔF/F responses to pulse song, calculated as $(F_{post} - F_{pre})/F_{pre}$, were roughly linear across a wide range of intensities; the 90 dB SPVL stimulus was chosen for further experiments (red cross; stimuli used 20 pulses per train).

(D) ΔF/F responses at 90 dB SPVL were a saturating function of pulse number; stimuli with 40 pulses per train (red cross) were chosen for further experiments.

(E and F) aPN1 response to pulse song in AMMC (E) and WED (F). Peak ΔF/F response increased linearly with decreasing IPI (solid line) but decreased abruptly at 20 ms IPI (dashed line; t test versus linear expectation, $p < 10^{-5}$ for both AMMC and WED, t test). Responses are normalized by the average response of each preparation at 65 ms IPI. Inset: raw responses at 25 ms and 65 ms IPI.

(G) Pairwise comparison AMMC and WED response across the linear response range. The WED ΔF/F response is damped at short IPIs and is well fit with an exponential squashing function ($R^2 = 0.85$, two-sample F test versus linear fit: $p = 0.001$; see Supplemental Information).

(H) Transfer function between AMMC and WED responses, normalized by average response. Compared to the AMMC response, the peak ΔF/F in WED is significantly enhanced at 35 ms IPI over both longer and shorter IPIs (Wilcoxon rank-sum test).

See also Figure S2. Error bars show mean ± SEM; *p < 0.05, **p < 0.01, ***p < 0.001.

band-pass filter for conspecific courtship song in a similar manner to the omega interneuron.

As a caveat, we note that the AMMC-WED modulation observed here appears relatively weak (10%–20%) and is the product of bulk recordings. Its underlying mechanism is unknown and may be explained by either intracellular mechanisms (such as presynaptic facilitation in WED) or circuit-level processes (such as presynaptic inhibition). Adding to this uncertainty, aPN1 has been reported to be nonspiking, which limits the effectiveness of intracellular recordings without paired recordings from (unknown) downstream targets [32]. Thus, although much progress has been made, localizing the precise mechanism of IPI discrimination remains an ongoing project.

Conclusions

Overall, these results demonstrate the considerable complexity of the antennomechanosensory circuits responsible for integrating a variety of multimodal mechanosensory stimuli. Among a variety of AMMC output pathways, the projection neuron aPN1, along with the aLN(al) interneuron, is critically necessary for the courtship response in both male and female flies. Moreover, the aPN1 response reflects a two-step filter that facilitates the detection and discrimination of courtship song. Our ongoing work will seek to identify the downstream pathway for courtship song processing and multimodal integration and the precise role of fru^M in the development and function of the auditory circuitry underlying species isolation in *D. melanogaster.*

Experimental Procedures

Identification of aPN and aLN Classes

Using data from the JFRC FlyLight project, we screened ~6,000 CRM-GAL4 lines for expression in the AMMC and categorized 288 AMMC lines into five aPN and seven aLN classes. Each class was identifiable in an average of 14 CRM lines, and a subset of lines with robust and specific on-target expression was selected for behavioral manipulation. Details of each cell type and CRM line are described in Figure S1 and Tables S1–S3.

Behavioral Manipulations

FR was observed over 20 min, with 15 min acclimatization before testing; minimum n = 48 pairs. SIL is the difference in expected and observed speed after presentation of synthetic song at 90 db SPVL and was performed with a minimum n = 50 pairs. For $shibire^{TS}$ and *dTrpA1* experiments, a significant interaction between genotype (test versus control) and temperature (permissive and restrictive) was assessed by the interaction term of a two-way Cox proportional hazards ANOVA or two-way ANOVA, respectively, for FR and SIL assays. Detailed statistical results are presented in Table S4.

Calcium Imaging

GCaMP3 was imaged at 488 nm at 13 Hz via a ventral window in six female flies. Song was presented at 90 dB SPVL from a loudspeaker 20 cm distant; the antenna and arista were free to move bilaterally. IPIs were presented

repeatedly in a pseudorandom order. Detailed protocols are provided in the Supplemental Experimental Procedures.

Supplemental Information

Supplemental Information includes Supplemental Experimental Procedures, two figures, and four tables and can be found with this article online at http://dx.doi.org/10.1016/j.cub.2014.03.048.

Acknowledgments

We dedicate this work in memory of R.M.H., and we thank Gerry Rubin, Arnim Jennet, Barret Pfeiffer, Karen Hibbard, Todd Laverty, and the FlyLight team for their work in creating the JFRC CRM collection; Vivek Jayaraman for assistance with GCaMP imaging; Tanya Tabachnik, Gus Lott, and Kristin Branson for engineering support; Crystal Sullivan and Allison Howard for administrative support; and all of the members of the JFRC community. A.G.V., C.Z., and B.S.B. were supported by HHMI.

Received: October 21, 2013
Revised: January 28, 2014
Accepted: March 17, 2014
Published: May 1, 2014

References

1. Sturtevant, A.H. (1915). Experiments on sex recognition and the problem of sexual selection in Drosophila. J. Anim. Behav. *5*, 351–366.
2. Markow, T.A., and O'Grady, P.M. (2005). Evolutionary genetics of reproductive behavior in Drosophila: connecting the dots. Annu. Rev. Genet. *39*, 263–291.
3. Manoli, D.S., Meissner, G.W., and Baker, B.S. (2006). Blueprints for behavior: genetic specification of neural circuitry for innate behaviors. Trends Neurosci. *29*, 444–451.
4. Bastock, M., and Manning, A. (1955). The courtship of Drosophila melanogaster. Behaviour *8*, 85–111.
5. Greenspan, R.J., and Ferveur, J.F. (2000). Courtship in Drosophila. Annu. Rev. Genet. *34*, 205–232.
6. Bennet-Clark, H.C., and Ewing, A.W. (1967). Stimuli provided by courtship of male Drosophila melanogaster. Nature *215*, 669–671.
7. von Philipsborn, A.C., Liu, T., Yu, J.Y., Masser, C., Bidaye, S.S., and Dickson, B.J. (2011). Neuronal control of Drosophila courtship song. Neuron *69*, 509–522.
8. Shorey, H.H. (1962). Nature of the sound produced by Drosophila melanogaster during courtship. Science *137*, 677–678.
9. Riabinina, O., Dai, M., Duke, T., and Albert, J.T. (2011). Active process mediates species-specific tuning of Drosophila ears. Curr. Biol. *21*, 658–664.
10. Bennet-Clark, H.C., and Ewing, A.W. (1969). Pulse interval as a critical parameter in the courtship song of Drosophila melanogaster. Anim. Behav. *17*, 755–759.
11. Ritchie, M.G., Halsey, E.J., and Gleason, J.M. (1999). Drosophila song as a species-specific mating signal and the behavioural importance of Kyriacou & Hall cycles in D. melanogaster song. Anim. Behav. *58*, 649–657.
12. Talyn, D., and Dowse, H. (2004). The role of courtship song in sexual selection and species recognition by female Drosophila melanogaster. Anim. Behav. *68*, 1165–1180.
13. Rybak, F., Aubin, T., Moulin, B., and Jallon, J.-M. (2002). Acoustic communication in Drosophila melanogaster courtship: are pulse-and sine-song frequencies important for courtship success? Can. J. Zool. *80*, 987–996.
14. Kyriacou, C., and Hall, J.C. (1982). The function of courtship song rhythms in Drosophila. Anim. Behav. *30*, 794–801.
15. von Schilcher, F. (1976). The function of pulse song and sine song in the courtship of Drosophila melanogaster. Anim. Behav. *24*, 622–625.
16. Bennet-Clark, H.C., Ewing, A.W., and Manning, A. (1973). The persistence of courtship stimulation in Drosophila melanogaster. Behav. Biol. *8*, 763–769.
17. Kowalski, S., Aubin, T., and Martin, J.-R. (2004). Courtship song in Drosophila melanogaster: a differential effect on male-female locomotor activity. Can. J. Zool. *82*, 1258–1266.
18. Crossley, S.A., Bennet-Clark, H.C., and Evert, H.T. (1995). Courtship song components affect male and female Drosophila differently. Anim. Behav. *50*, 827–839.
19. von Schilcher, F. (1976). The role of auditory stimuli in the courtship of Drosophila melanogaster. Anim. Behav. *24*, 18–26.
20. Kamikouchi, A., Inagaki, H.K., Effertz, T., Hendrich, O., Fiala, A., Göpfert, M.C., and Ito, K. (2009). The neural basis of Drosophila gravity-sensing and hearing. Nature *458*, 165–171.
21. Eberl, D.F., Duyk, G.M., and Perrimon, N. (1997). A genetic screen for mutations that disrupt an auditory response in Drosophila melanogaster. Proc. Natl. Acad. Sci. USA *94*, 14837–14842.
22. Nadrowski, B., Effertz, T., Senthilan, P.R., and Göpfert, M.C. (2011). Antennal hearing in insects—new findings, new questions. Hear. Res. *273*, 7–13.
23. Yorozu, S., Wong, A., Fischer, B.J., Dankert, H., Kernan, M.J., Kamikouchi, A., Ito, K., and Anderson, D.J. (2009). Distinct sensory representations of wind and near-field sound in the Drosophila brain. Nature *458*, 201–205.
24. Lehnert, B.P., Baker, A.E., Gaudry, Q., Chiang, A.-S., and Wilson, R.I. (2013). Distinct roles of TRP channels in auditory transduction and amplification in Drosophila. Neuron *77*, 115–128.
25. Kamikouchi, A., Shimada, T., and Ito, K. (2006). Comprehensive classification of the auditory sensory projections in the brain of the fruit fly Drosophila melanogaster. J. Comp. Neurol. *499*, 317–356.
26. Manoli, D.S., Foss, M., Villella, A., Taylor, B.J., Hall, J.C., and Baker, B.S. (2005). Male-specific *fruitless* specifies the neural substrates of *Drosophila* courtship behaviour. Nature *436*, 395–400.
27. Stockinger, P., Kvitsiani, D., Rotkopf, S., Tirián, L., and Dickson, B.J. (2005). Neural circuitry that governs Drosophila male courtship behavior. Cell *121*, 795–807.
28. Cachero, S., Ostrovsky, A.D., Yu, J.Y., Dickson, B.J., and Jefferis, G.S.X.E. (2010). Sexual dimorphism in the fly brain. Curr. Biol. *20*, 1589–1601.
29. Lai, J.S.-Y., Lo, S.-J., Dickson, B.J., and Chiang, A.-S. (2012). Auditory circuit in the Drosophila brain. Proc. Natl. Acad. Sci. USA *109*, 2607–2612.
30. Yu, J.Y., Kanai, M.I., Demir, E., Jefferis, G.S.X.E., and Dickson, B.J. (2010). Cellular organization of the neural circuit that drives Drosophila courtship behavior. Curr. Biol. *20*, 1602–1614.
31. Lin, S., Kao, C.-F., Yu, H.-H., Huang, Y., and Lee, T. (2012). Lineage analysis of Drosophila lateral antennal lobe neurons reveals notch-dependent binary temporal fate decisions. PLoS Biol. *10*, e1001425.
32. Tootoonian, S., Coen, P., Kawai, R., and Murthy, M. (2012). Neural representations of courtship song in the Drosophila brain. J. Neurosci. *32*, 787–798.
33. Jenett, A., Rubin, G.M., Ngo, T.-T.B., Shepherd, D., Murphy, C., Dionne, H., Pfeiffer, B.D., Cavallaro, A., Hall, D., Jeter, J., et al. (2012). A GAL4-driver line resource for Drosophila neurobiology. Cell Rep *2*, 991–1001.
34. Hampel, S., Chung, P., McKellar, C.E., Hall, D., Looger, L.L., and Simpson, J.H. (2011). Drosophila Brainbow: a recombinase-based fluorescence labeling technique to subdivide neural expression patterns. Nat. Methods *8*, 253–259.
35. Kohatsu, S., Koganezawa, M., and Yamamoto, D. (2011). Female contact activates male-specific interneurons that trigger stereotypic courtship behavior in Drosophila. Neuron *69*, 498–508.
36. Liu, W., Liang, X., Gong, J., Yang, Z., Zhang, Y.-H., Zhang, J.-X., and Rao, Y. (2011). Social regulation of aggression by pheromonal activation of Or65a olfactory neurons in Drosophila. Nat. Neurosci. *14*, 896–902.
37. Pan, Y., Robinett, C.C., and Baker, B.S. (2011). Turning males on: activation of male courtship behavior in Drosophila melanogaster. PLoS ONE *6*, e21144.
38. Zhou, C., Rao, Y., and Rao, Y. (2008). A subset of octopaminergic neurons are important for Drosophila aggression. Nat. Neurosci. *11*, 1059–1067.
39. Tian, L., Hires, S.A., Mao, T., Huber, D., Chiappe, M.E., Chalasani, S.H., Petreanu, L., Akerboom, J., McKinney, S.A., Schreiter, E.R., et al. (2009). Imaging neural activity in worms, flies and mice with improved GCaMP calcium indicators. Nat. Methods *6*, 875–881.
40. Heeger, D.J. (1992). Normalization of cell responses in cat striate cortex. Vis. Neurosci. *9*, 181–197.
41. Olsen, S.R., Bhandawat, V., and Wilson, R.I. (2010). Divisive normalization in olfactory population codes. Neuron *66*, 287–299.

42. Fabre, C.C.G., Hedwig, B., Conduit, G., Lawrence, P.A., Goodwin, S.F., and Casal, J. (2012). Substrate-borne vibratory communication during courtship in Drosophila melanogaster. Curr. Biol. *22*, 2180–2185.
43. Robert, D., Amoroso, J., and Hoy, R.R. (1992). The evolutionary convergence of hearing in a parasitoid fly and its cricket host. Science *258*, 1135–1137.
44. Eyherabide, H.G., Rokem, A., Herz, A.V.M., and Samengo, I. (2008). Burst firing is a neural code in an insect auditory system. Front Comput Neurosci *2*, 3.